Modeling and Optimization of Visible Light Carrierless Amplitude and Phase Modulation Links

Kerem Enhos, Emrecan Demirors, Deniz Unal and Tommaso Melodia Institute for The Wireless Internet of Things, Northeastern University, Boston, MA, USA Email: {enhos.k, e.demirors, unal.d, melodia}@northeastern.edu

Abstract—Carrierless Amplitude and Phase (CAP) modulation has been widely used in the emerging visible light communication (VLC) paradigm. Compared to other modulation schemes, CAP is in fact known to be comparatively easy to implement, to have lower computational complexity, high spectral efficiency, and superior noise performance. However, as of today, how to select optimal parameters in CAP links for a desired target bit error rate (BER) performance and spectral efficiency requirements is still an open problem, because of the absence of closed-form expressions for the bit error probability under different signalto-noise ratio (SNR) conditions. In this article, we present a comprehensive analysis on the impact of different CAP parameters on the bit error probability under different noise levels. We first describe the system model and derive a theoretical expression for the bit error rate of a CAP-modulated communication system. Then, we present detailed simulation and experimental results for different CAP parameters. The derived theoretical expression is also validated through simulations and experiments for each different CAP parameter. Then, with this expression, we show how to select optimal link parameters for different noise levels, by maximizing the spectral efficiency while keeping the BER lower than a predefined threshold.

Index Terms—CAP Modulation, Visible Light Communication, Software-Defined Modem.

I. INTRODUCTION

Wireless communication systems are exponentially growing in the need of bandwidth and high-speed in radio-frequency (RF) domain. Especially, competition for spectrum allocation and licensing pose problems for both development of internetof-things systems and wireless communication market [1]. These problems result in a search for alternative communication domains, such as visible light. With the emerging and promising advantages of visible light communication (VLC) technology, high-speed, robust and unlicensed communication systems can be implemented [2]-[4]. VLC technology also draws attention for future 6G networks, where reconfigurable and flexible software-defined optical systems can enhance the next generation of networks [5]. However, VLC systems are distinct from RF domain, where conventional physical layers are employing coherent, multi order and spectrally efficient modulation schemes. These differences and advancement opportunities in VLC technology, led to development of networking standards for VLC in IEEE 802.15.7 [6] and IEEE 802.11bb [7]. Hence, alternative modulation schemes

Acknowledgement: This work was supported by the National Science Foundation under Grant CNS-1763964 and Grant CNS-1726512.

that satisfy the physical requirements of visible light domain have been proposed for VLC.

Carrierless amplitude and phase modulation (CAP) is a spectrally efficient, multi-band capable, multi-order physical layer scheme that is used for intensity modulation and directdetection (IM/DD). Because of the non-coherent nature of visible light communication (VLC), conventional physical layers used in RF domain cannot be applied in optical communication links and transmitted/received signals should be positive and real valued. Thus, with its ease of implementation and lower computational complexity depending on its parameter selection, CAP is widely used for VLC. While it provides higher spectral efficiency and noise performance compared to singlecarrier modulation schemes (such as OOK, PPM, among others), it also outperforms other multi-carrier modulation schemes (MCM), which are denoted as discrete multi-tone (DMT) in terms of susceptibility to noise and PAPR factors [8]. Overall, despite its sensitivity to timing jitter, CAP has the advantage of lower PAPR and lower BER over other multicarrier modulation (MCM) schemes at the same data rate. In VLC, as transmitting sources LEDs are widely used, because of its low cost, accessibility and low power consumption. However, LEDs suffer from low modulation bandwidth and non-linearity. In order to efficiently use this bandwidth and increase the spectral efficiency to achieve higher data rates, multi-carrier modulation schemes, such as CAP, need to be used.

While there have been multiple research efforts on using CAP modulation, a comprehensive and detailed analysis of the parameters that affect the performance of CAP modulation have not been presented. Efficient usage and modification of these parameters affect the data rate, spectral efficiency, computational complexity and peak-to-average power (PAPR) usage. By configuring CAP parameters in real-time according to the channel properties (such as noise power, multipath, etc.), more efficient, robust, and sustainable communication links can be maintained. However, this adaptive configuration requires knowledge on the effect of CAP parameters or efficient calculation of communication properties. With the usage of software-defined radio paradigm; reconfigurable, self-optimizing and adaptive CAP modulated VLC links can be implemented.

To address these challenges, in this paper, we propose an empirically derived theoretical expression for bit error probability of M-QAM encoded CAP modulation under different noise power levels in Section II. Then in Section III, comprehensive analysis on the effect of different parameters of pulse shaping filters and CAP modulation are presented along with the validation of the theoretical expression of each parameter with the simulated data. Furthermore, preliminary experimental results are also used for cross-validation of the proposed expression and system, which is explained in Section IV. Finally, in Section V, it is shown that effective configuration of these parameters can be used for software defined optical modems with real-time adaptation capabilities by selecting the optimal parameters of CAP modulation under different channel properties.

II. SYSTEM MODEL

In CAP modulation, each incoming binary data bit is mapped in M-QAM constellations, denoted as A_i . In-phase and quadrature components are filtered with a root raised cosine (RRC) filter which is multiplied with cosine and sine functions respectively for each component of this complex symbol. These filters construct a Hilbert pair, which are orthogonal with same amplitude and 90° phase difference [9]. After filtering, both components are summed and by adding DC bias, signal can be transmitted with LED. Hence, the resulting transmitted signal can be shown as:

$$x_{CAP}(t) = \sum_{i=-\infty}^{\infty} \left[\operatorname{Re}(A_i) f_I(t-iT) - \operatorname{Im}(A_i) f_Q(t-iT) \right]$$

where pulse-shaping filters, f_I and f_Q , are denoted as:

$$f_I(t) = g_{RRC}(t)\cos(2\pi f_c t),\tag{2}$$

and

$$f_O(t) = q_{RRC}(t)\sin(2\pi f_c t),\tag{3}$$

where g_{RRC} is the root raised cosine function. Finally, the summation of these signals result in real valued waveform, which can be transmitted through appropriate DC bias through VLC front-ends. After receiving the intensity modulated signal through the visible light channel, real valued signal is again filtered through the matched f_I and f_Q filters. Finally, these two parts are superposed to form the complex signal, which then be downsampled and decoded through relevant M-QAM.

For multi-band version of CAP modulation, which is denoted as m-CAP, can be implemented with the same principle by only changing the center frequency of the f_I and f_Q filters and then superposing the resulting waveforms for each subband [10]. With this property, higher data rates and reliability can be obtained for frequency selective channels. It is important to note that the bandwidth of each sub-band is dictated through the samples-per-symbol (N_{ss}) and roll-off factor (α) . Sampling frequency at which the m-CAP signals are generated has to be higher than the Nyquist rate, where the signals can be recovered correctly [11]. Hence, in order to maintain this requirement, N_{ss} has to be adjusted accordingly, for a given number of sub-bands (m) and α , as given in eq. (4).

$$N_{ss} > \lceil 2m \left(1 + \alpha \right) \rceil \tag{4}$$

By appropriate selection of RRC parameters, such as span (S_p) , N_{ss} , roll-off factor, modulation order (M) and number of sub-bands, spectral efficiency of this modulation scheme can be adjusted. For low SNR values, selection of higher S_n or N_{ss} values can results in better BER with the drawback of higher implementation complexity, longer filter length and lower data rate. Length of the pulse shaping filter is dictated by S_n , N_{ss} , and roll-off factor. Thus, as these values increase, data rate will decrease and for real time implementations on FPGAs or DSPs, complexity will increase. On the other hand by increasing the number of sub-bands or the modulation order, data rate can be highly increased with same utilized bandwidth compared to conventional pulse time modulation (PTM) schemes. Thus, it can be concluded that changing the pulse shaping filter parameters, number of sub-bands or modulation order, can result in better communication performance of the VLC link for different signal-to-noise ratio (SNR) levels in terms of bit-error-rate (BER) at a given utilized bandwidth. Although this alteration results in different spectral efficiency for a given SNR level of the communication channel, best possible parameter combination can be calculated by having minimum BER at highest possible spectral efficiency. Thus, an adaptive communication system with optimum parameters for time variant channels can be implemented.

In order to determine this optimum selection, communication system can be simulated through MATLAB, where the VLC channel can be modeled as AWGN channel. By using the same principle described in Fig. 1, random generated bits can be modulated in CAP modulation scheme to be transmitted through an AWGN channel, where noise level is computed and added to obtain desired SNR level. Although this system is computationally cheaper compared to other MCM schemes, still computing high number of random generated bits ($> 10^6$) with different seeds, is highly time consuming and infeasible for real-time adaptive communication simulation systems. In order to compute the optimum CAP parameters for a given SNR level at desired minimum BER, a theoretical representation is needed. With this theoretical representation both BER and spectral efficiency can be calculated for each CAP parameter to adjust the communication system adaptively to the VLC channel in real-time.

A generalized closed-form bit error probability expression of gray coded square M-ary QAM bit mapping is derived in [12], for AWGN channels. This generalized conditional bit error probability corresponding to the k-th bits can be expressed as

$$P_{b}(k) = \frac{1}{\sqrt{M}} \sum_{j=0}^{\left(1-2^{-k}\right)\sqrt{M}-1} \left[(-1)^{\left\lfloor \frac{j\cdot2^{k-1}}{\sqrt{M}} \right\rfloor} \cdot \left(2^{k-1} - \left\lfloor \frac{j\cdot2^{k-1}}{\sqrt{M}} + \frac{1}{2} \right\rfloor \right)$$

$$\cdot erfc\left((2\cdot j+1)\sqrt{\frac{3\log_{2}M \cdot \gamma_{SNR}}{2(M-1)}} \right) \right]$$
(5)

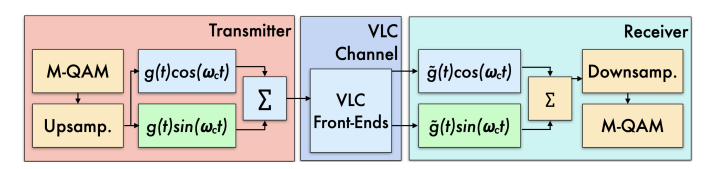


Fig. 1. Block diagram of carrierless amplitude and phase modulation scheme.

where $k = 1, 2, 3, ..., \log_2 \sqrt{M}$. Finally, exact bit error probability of M-QAM, P_b , for $M = 2^N$ where N is even, can be obtained by

$$P_b = \frac{1}{\log_2 \sqrt{M}} \sum_{k=1}^{\log_2 \sqrt{M}} P_b(k).$$
 (6)

Though, eq. (6) is the expression for M-QAM, by modifying the linear SNR term, γ_{SNR} , given in eq. (5), same bit error probability expression for m-CAP modulation can be obtained. Empirically derived BER expression for m-CAP modulation is asserted by using eq. (5) and eq. (6) by defining $\overline{\gamma_{SNR}}$ as

$$\overline{\gamma_{SNR}} = \gamma_{SNR} \times \left[\frac{(S_p \cdot N_{ss} + 1)}{2m \cdot \log_2 M} \right], \tag{7}$$

where N_{ss} is selected accordingly to eq. (4). Thus, by only replacing the linear SNR term in eq. 5 with $\overline{\gamma_{SNR}}$, m-CAP bit error probability can be calculated for different CAP parameters. Also $(S_p \cdot N_{ss} + 1)$ term is equal to the filter length of the RRC pulse shaping filter. This expression given in eq. (7) can be comprehended intuitively since increasing the filter length, which is the numerator of the SNR term, should increase SNR for matching filters. Similarly, increasing the modulation order or the number of sub-bands increases the requirement of higher SNR for lower bit errors.

III. NUMERICAL RESULTS

In this section, we present the results of different CAP parameters that affect the communication link with MATLAB simulations. Also by providing the theoretical results with the extensive Monte-Carlo simulations of CAP communication system described in Section II, validation of the theoretical expression given in eq. (5)-(7) is conducted.

Transmitted waveforms are superposed with appropriate noise power levels to obtain desired SNR. For each set of parameters 10⁹ random bits are fed into the system in order to assess lower bit error probability. Monte-Carlo simulations are conducted by executing the communication system by 100 times with different random seeds for the generation of random binary bits and average error probability for each SNR level is presented.

Both simulation and theoretical expression validation results are presented for different values of span (S_p) , samples-persymbol (N_{ss}) , roll-off factor (α) , modulation order (M) and number of sub-bands (m).

A. Span (S_n)

Firstly, span values are differentiated between 2, 4, 8, 16, and 40, while keeping other parameters at M=16, $\alpha=0.1$,

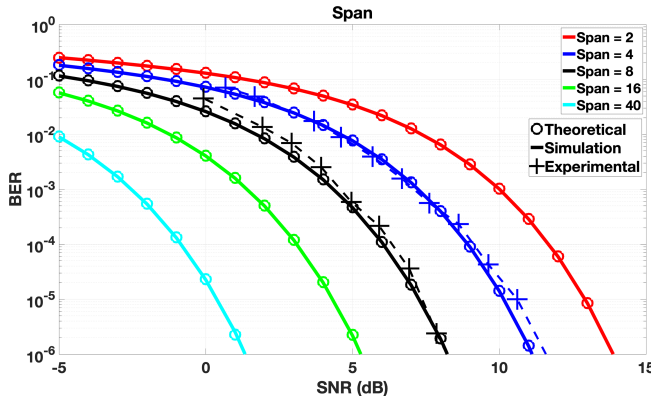


Fig. 2. BER results of theoretical and simulated data for different span values, while M=16, $\alpha=0.1$, m=1, and $N_{ss}=4$. Theoretical values are represented in solid lines and simulated results are shown in circles.

m=1, and $N_{ss}=4$. In Fig. 2, impact of different S_p values of the RRC filter used in pulse shaping filters of CAP modulation is shown along with the theoretical expression results. As S_p increases, noise performance in terms of BER also increases. Since span value corresponds to the truncation term of the RRC filter, filter length also increases, where at span value of 40, filter length is equal to 81, complexity of the system also increases and data rate decreases. However, at SNR level of $2\,\mathrm{dB}$, BER lower than 10^{-6} can be obtained with $0.0988\,\mathrm{bit/s/Hz}$ spectral efficiency. Effect of span values on the frequency response of the RRC filter can be found in [9].

B. Samples-per-symbol (N_{ss})

As the parameter that affects the filter length and the bandwidth of the pulse shaping filter, samples-per-symbol (N_{ss}) , has an important impact on the CAP modulated communication systems. Again, N_{ss} , is values of 2, 4, 8, and 12 are selected for the CAP system that set with M=16, $\alpha=0.1$, m=1, and $S_p=4$. In Fig. 3, impact of different N_{ss} values are shown for different noise levels. Theoretical expression is also validated with simulation data. Also in this figure, N_{ss} , value that violates eq. (4) is also given. Although, this bandwidth allocation violates the Nyquist criteria as explained in Section II and noise performance decreases, still successful communication link can still be obtained for higher SNR levels. Also, theoretical expression slightly deviates from the simulated data for lower bit error probabilities since given expression assumes that each pulse shaping filter in the system relies on the Nyquist ISI criterion.

C. Roll-off Factor (α)

Another parameter that affects the bandwidth of the communication system is the roll-off factor that is denoted as α . Similarly to any filtering circuit, as the α increases, steepness of the transition between the passband and the stopband of the filter decreases, which result in narrower passband and lower spectral efficiency for the communication system. For RRC filter, this value spans between 0 and 1. Thus, in order to observe the affect of α , values of 0.1, 0.5, and 0.9

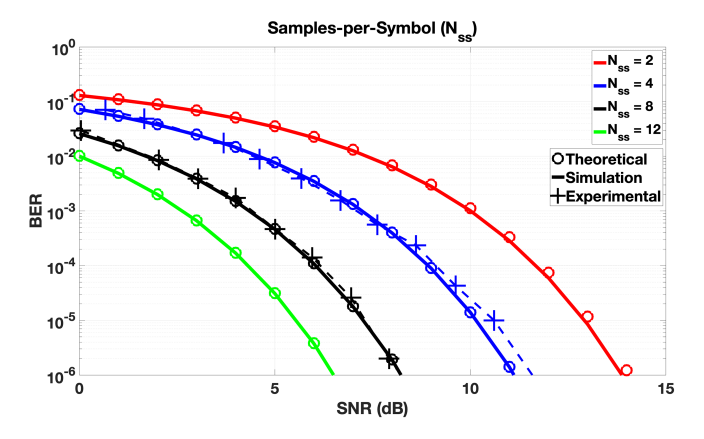


Fig. 3. BER results of theoretical and simulated data for different N_{ss} values, while $M=16,\,\alpha=0.1,\,m=1,$ and $S_p=4.$ Theoretical values are shown in solid lines and simulated results are shown in circles.

are selected while keeping other parameters at M=16, m=1, and $S_p=4$. According to eq. (4), N_{ss} depends on α , thus for the aforementioned α values, N_{ss} values are selected to be 4, 5, and 6 respectively. In Fig. 4, impact of different α values are shown for different SNR levels. Similarly, theoretical expression is validated with the simulated data. Although, a dramatic noise performance deviation is not observed for different roll-off factor, as α increases noise performance gets better while lowering the spectral efficiency from $0.47 \, \mathrm{bit/s/Hz}$ to $0.32 \, \mathrm{bit/s/Hz}$ for α values of 0.1 and 0.9 respectively.

D. Modulation Order (M)

Modulation order (M) of the M-ary QAM system greatly impacts the spectral efficiency and noise performance of the communication links. For very high SNR scenarios ($> 25 \, \mathrm{dB}$), high M values (e.g., 256, 1024) can be selected, however, in due to multipath, ISI, distortions or non-linearity of the communication system, these values may be challenging for robust and reliable real world VLC applications and systems. Thus, by selecting moderate and common M values of 4, 16, and 64 for the QAM system, impact of modulation order on

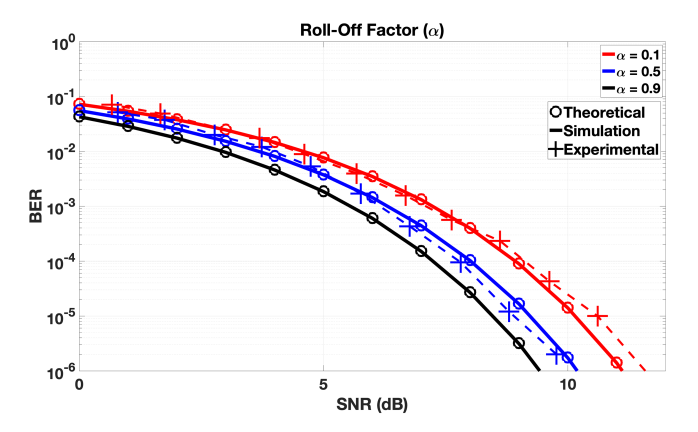


Fig. 4. BER results of theoretical and simulated data for different α values of 0.1, 0.5 and 0.9, while $M=16, m=1, S_p=4$ and N_{ss} equals to 4, 5, and 6 respectively. Theoretical values are shown in solid lines and simulated results are shown in circles.

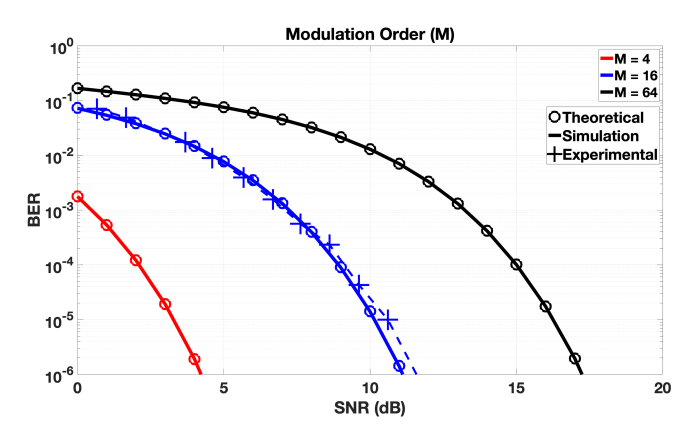


Fig. 5. BER results of theoretical and simulated data for different modulation orders, M, while $N_{ss}=4$, $\alpha=0.1$, m=1, and $S_p=4$. Theoretical values are represented in solid lines and simulated results are shown in circles.

the noise performance of the CAP communication system is observed while keeping other parameters at $\alpha=0.1,\,N_{ss}=4,\,m=1,\,$ and $S_p=4.$ Unlike other filter parameters, M has the greatest impact on both the noise performance and the spectral efficiency. With the given parameters, successful communication links can be maintained for very low SNR scenarios at M=4. Theoretical expression is again validated for M with the simulated data and this validation can be further extended to higher modulation orders, where M is obtained from $M=2^N$ where N is even.

E. Sub-bands (m)

Lastly, noise performance of different number of sub-bands are observed for m values of 1, 3, 5, and 10, while selecting other parameters as $\alpha = 0.1$, M = 16, and $S_p = 4$. Also according to eq. (4), N_{ss} depends on m, so for the aforementioned m values, N_{ss} values are selected to be 4, 9, 13, and 24 respectively. As it is shown in Fig. 6, as the number of sub-bands increase, higher SNR level is required in order to maintain same BER. However, spectral efficiency increases as m increases, which is also advantageous for frequency selective communication channels since existing bandwidth can be utilized more efficiently. While spectral efficiency is equal to 0.47bit/s/Hz for single sub-band usage of CAP modulation, spectral efficiency increases to 0.83 bit/s/Hz for 10-CAP. On the other hand, increasing the number of sub-bands also increases PAPR, which is an important consideration for digital wireless communication systems. For single sub-band utilized CAP modulation system has a PAPR of 9.21, for 10-CAP system this ratio increases to 16.04. Finally, theoretical expression is validated for m with the simulated data as it is given in Fig. 6.

IV. EXPERIMENTAL RESULTS

In addition to the detailed simulation results, we have conducted a preliminary experimental study to validate the presented closed-form expression, which are also shown in Figures 2-6 for different CAP parameters. All experiments are conducted in a dark room, where transmitter and receiver are placed 7 m apart from each other, and optical signals

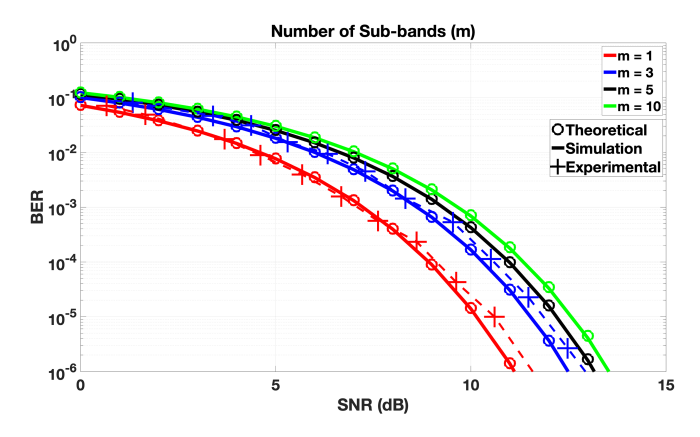


Fig. 6. BER results of theoretical and simulated data for different m values of 1, 3, 5, and 10, while M=16, $\alpha=0.1$, $S_p=4$ and N_{ss} equals to 4, 9, 13, and 24 respectively. Theoretical values are shown in solid lines and simulated results are shown in circles.

are propagated over the air. Experiments are conducted by using software-defined VLC modem introduced in [8], where detailed information is presented. This modem is designed and built on software-defined radio paradigm for its configurability and adaptive communication capabilities. Hence, this capability offers the implementation and transmission of different CAP parameter configurations with this modem for different corresponding channel configurations. During the experiments, $1 \mathrm{MHz}$ of bandwidth is utilized. SNR of each received packet is calculated in frequency domain due to the fact that higher N_{ss} or α values narrow down the signal bandwidth and SNR has to be calculated according to the transmitted signal bandwidth.

In Fig. 2-6, experimental data for different span, N_{ss} , rolloff factor, modulation order and number of sub-bands are shown in dashed lines with plus markings. It is shown that the experimental data also cross-validates both the simulation and theoretical expression. Since, both simulation and theoretical expression only takes AWGN channels into consideration, other noise and distortion components that can be generated through the non-linearity of transmitter and receiver circuitry adjusted to be minimum for a fair validation. Due to the fact that simulation data is collected through Monte-Carlo simulations with different seeds for each iteration, lower bit error probabilities ($< 10^{-5} BER$) converges to the theoretical expression. However, experimental data has a higher error margin for these low BER values as it can be seen from the figures. Also for the briefness of this manuscript, number of CAP parameter configurations are kept limited.

As a result, both the simulation system and the proposed theoretical expression are cross-validated with these set of experiments by configuring the system with different CAP parameters. This cross-validation can also be further extended to different mediums and channels. By inputting the relevant channel (underwater, air-water interface, etc.) response, similarly as shown in [8], in the simulation system, communication link analysis can be executed for different mediums.

V. OPTIMAL PARAMETER SELECTION

Previously, spectral efficiency differentiation by different selection of CAP parameters were mentioned. For given BER or spectral efficiency constraints, CAP parameters can be adjusted to perform accordingly. Given that both the spectral efficiency and bit error probability of CAP modulated systems are functions, which are depending on CAP parameters discussed in Section III, optimal system configurations can be obtained by numerically calculating different selections. Spectral efficiency, for CAP modulation, is given as

$$f(S_p, N_{ss}, \alpha, M, m) = \frac{2 \cdot m \cdot \log_2 M}{S_p \cdot N_{ss} + 1},$$
 (8)

where N_{ss} , must satisfy the inequality given in eq. (4). It may be seen that α value only affects the minimum selection of N_{ss} for the calculation of spectral efficiency. Leveraging the spectral efficiency definition of CAP modulation and presented closed-form expression for bit error probability of CAP modulation, a parameter selection algorithm can be formulated. The parameter selection algorithm has the objective to maximize the spectral efficiency at a given SNR value $(\overline{\gamma_{SNR}})$ while satisfying a maximum acceptable bit error probability (\hat{P}) by selecting Span (S_p) , samples per symbol (N_{ss}) , roll-off factor (α) , modulation order (M) and number of sub-bands (m). Given that $S_{p,max}$, $N_{ss,max}$, M_{max} , and m_{max} are the maximum span, samples-per-symbol, modulation order and number of sub-bands supported, the optimization objective can be expressed as

given
$$\overline{\gamma_{SNR}}$$
 (9)

$$\underset{S_p, N_{ss}, \alpha, M, m}{\text{maximize}} f(S_p, N_{ss}, \alpha, M, m) \tag{10}$$

subject to
$$P_b(S_p, N_{ss}, \alpha, M, m) < \hat{P}$$
 (11)

$$0 < S_p \le S_{p,max}, \ S_p \in \mathbb{N} \tag{12}$$

$$0 < N_{ss} \le N_{ss,max}, \ N_{ss} \in \mathbb{N}$$
 (13)

$$0 < M \le M_{max}, \ M \in \mathbb{N}$$
 (14)

$$0 < m \le m_{max}, \ m \in \mathbb{N}, \tag{15}$$

$$0 < \alpha < 1, \ m \in \mathbb{R},\tag{16}$$

$$(4) (17)$$

where \mathbb{N} and \mathbb{R} are the set of natural and real numbers, respectively. The problem stated in (10) is a mixed integer problem, i.e., all variables except α are integer variables, where a Branch and Bound method can be used for solution.

Finally, in order to visualize a possible solution set for the optimization problem presented in Eq. (10) for a given SNR level, comprehensive simulation and validation of theoretical formulation is performed with wide range of different CAP parameters. In Fig. 7, simulated data points and theoretical results are shown in circles and dots respectively for a communication link at 0 dB SNR level.

It can be observed that separate curves are resulted in Fig. 7, which denotes different modulation orders. As the modulation order increases, higher spectral efficiency can be

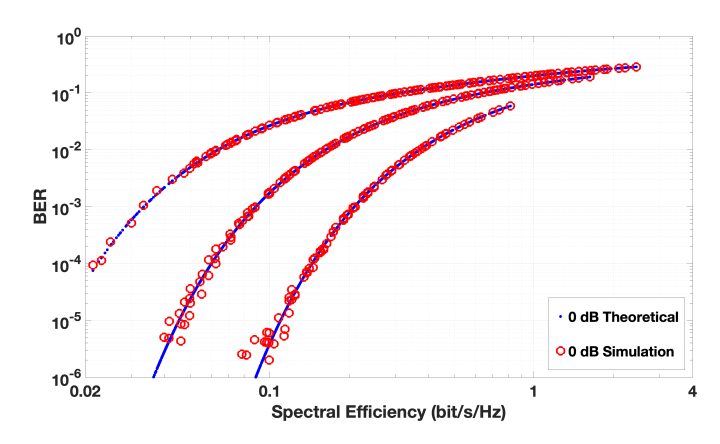


Fig. 7. Wide range of CAP parameters are simulated and cross-validated with theoretical results at 0 dB SNR. BER and their corresponding spectral efficiencies are obtained for each selection of CAP parameters.

maintained, however, dramatic increase on BER also occurs. Thus, increasing modulation order to enhance the data rate may not be the best solution to pursue in CAP systems. Validation of the theoretical expression with the simulated data implies that this solution can be further extended to real-time applications for adaptive and self-optimizing communication systems. Also by observing the resulting curves, it is clear that an optimal solution of CAP parameters, which maximizes the spectral efficiency for a given upper limit of bit error probability.

Similar implementation of this optimal parameter selection problem solution with different set of constraints can be useful for different applications. For bandwidth limited systems or communication links where communication can be maintained through spectrum holes, bandwidth of the CAP system constrained by N_{ss} , roll-off factor and circuitously number of sub-bands. Thus, setting constant parameters on bandwidth selection and differentiating other filter parameters that affect BER and spectral efficiency, set of optimal or suboptimal solutions can be determined. Similarly, for different constraints or applications such as maximizing throughput, minimizing BER, bandwidth limited communication link, etc., different problem sets can be determined and solved through the usage of the proposed theoretical expression. Also suboptimal solution set can be obtained through maximin problem formulation by determining the feasible solution set for maximum spectral efficiency and BER lower than the upper limit of error probability.

VI. CONCLUSIONS

We presented the impact of different system parameters of CAP modulation scheme with comprehensive bit error probability analysis under different noise conditions. Also by including the empirically derived theoretical bit error probability expression for M-QAM encoded and CAP modulated system, optimal parameter selection for maximum acceptable BER and minimum desired spectral efficiency under different noise levels can be obtained. This expression provides flexibility of calculating detailed numerical solution for different channel configurations, which prevents exhausting and time

consuming simulations. Also, ability to calculate the optimal parameters of CAP modulated system is immensely beneficial for adaptation capable communication systems, such as software-defined networks. As the future work, after obtaining comprehensive analysis and observing the effect of different system parameters, an adaptive VLC system that can solve the aforementioned optimization problem according to the communication channel and adjust its' system parameters according to the relevant solution, which employs CAP modulation scheme will be implemented with a software-defined radio manner.

REFERENCES

- [1] M. R. Palattella, M. Dohler, A. Grieco, G. Rizzo, J. Torsner, T. Engel, and L. Ladid, "Internet of things in the 5g era: Enablers, architecture, and business models," *IEEE Journal on Selected Areas in Communications*, vol. 34, no. 3, pp. 510–527, 2016.
- [2] P. H. Pathak, X. Feng, P. Hu, and P. Mohapatra, "Visible light communication, networking, and sensing: A survey, potential and challenges," *IEEE Communications Surveys Tutorials*, vol. 17, no. 4, pp. 2047–2077, 2015.
- [3] N. Cen, J. Jagannath, S. Moretti, Z. Guan, and T. Melodia, "Lanet: Visible-light ad hoc networks," Ad Hoc Networks, vol. 84, pp. 107–123, 2019
- [4] N. Cen, N. Dave, E. Demirors, Z. Guan, and T. Melodia, "Libeam: Throughput-optimal cooperative beamforming for indoor visible light networks," in *IEEE INFOCOM 2019 - IEEE Conference on Computer Communications*, April 2019, pp. 1972–1980.
- [5] M. Z. Chowdhury, M. Shahjalal, M. K. Hasan, and Y. M. Jang, "The role of optical wireless communication technologies in 5g/6g and iot solutions: Prospects, directions, and challenges," *Applied Sciences*, vol. 9, no. 20, 2019. [Online]. Available: https://www.mdpi.com/2076-3417/9/20/4367
- [6] M. Uysal, F. Miramirkhani, O. Narmanlioglu, T. Baykas, and E. Panayirci, "IEEE 802.15.7r1 reference channel models for visible light communications," *IEEE Communications Magazine*, vol. 55, no. 1, pp. 212–217, 2017.
- [7] IEEE, "IEEE standard p802.11bb," IEEE Standard for Information Technology—Telecommunications and Information Exchange Between Systems Local and Metropolitan Area Networks—Specific Requirements Part 11: Wireless LAN Medium Access Control (MAC) and Physical Layer (PHY) Specifications—Amendment: Light Communications, p. 1, 2018.
- [8] K. Enhos, E. Demirors, D. Unal, and T. Melodia, "Software-defined visible light networking for bi-directional wireless communication across the air-water interface," in 2021 18th Annual IEEE International Conference on Sensing, Communication, and Networking (SECON), 2021, pp. 1–9.
- [9] K. O. Akande, P. A. Haigh, and W. O. Popoola, "On the implementation of carrierless amplitude and phase modulation in visible light communication," *IEEE Access*, vol. 6, pp. 60532–60546, 2018.
- [10] P. A. Haigh, S. T. Le, S. Zvanovec, Z. Ghassemlooy, P. Luo, T. Xu, P. Chvojka, T. Kanesan, E. Giacoumidis, P. Canyelles-Pericas, H. L. Minh, W. Popoola, S. Rajbhandari, I. Papakonstantinou, and I. Darwazeh, "Multi-band carrier-less amplitude and phase modulation for bandlimited visible light communications systems," *IEEE Wireless Communications*, vol. 22, no. 2, pp. 46–53, 2015.
- [11] M. I. Olmedo, T. Zuo, J. B. Jensen, Q. Zhong, X. Xu, S. Popov, and I. T. Monroy, "Multiband carrierless amplitude phase modulation for high capacity optical data links," *Journal of Lightwave Technology*, vol. 32, no. 4, pp. 798–804, 2014.
- [12] D. Yoon, K. Cho, and J. Lee, "Bit error probability of m-ary quadrature amplitude modulation," in Vehicular Technology Conference Fall 2000. IEEE VTS Fall VTC2000. 52nd Vehicular Technology Conference (Cat. No.00CH37152), vol. 5, 2000, pp. 2422–2427 vol.5.